Supporting Information

# Lithiophilic Sn-Co nano-seeds sealed in hollow carbon shell to stabilize lithium metal anodes

Qiuping Li‡[a], Jiaming Zhang‡[a], Yaping Zeng[a], Zheng Tang[a], Dan Sun[a], Zhiguang Peng*[a], Yougen Tang[a,b], Huanhuan Li,[c] Haiyan Wang*[a,b]

*Corresponding author.

a. Hunan Provincial Key Laboratory of Chemical Power Sources, College of Chemistry and Chemical Engineering, Central South University, Changsha, 410083, P.R China. E-mail: wanghy419@csu.edu.cn; zhgpeng@csu.edu.cn.

b. Shenzhen Research Institute of Central South University, Shenzhen, 518057, P.R China.

c. School of Chemistry and Chemical Engineering, Henan Normal University, Xinxiang 453007, P. R. China.

‡ These authors contributed equally to this work.

**Preparation of $CoSn(OH)_6$ nanocubes:** 1 mmol of stannic chloride hydrated ($SnCl_4 \cdot 5H_2O$) was dissolved in 5 mL of ethanol (EA) (named as solution A). Besides, 1 mmol cobalt chloride hexahydrate ($CoCl_2 \cdot 6H_2O$) and 0.294 g sodium citrate dihydrate ($C_6H_5Na_3O_7 \cdot 2H_2O$) were dissolved in 20 mL deionized water (DIW) to obtain a homogeneous solution (named as solution B). 1.60 g sodium hydroxide (NaOH) was dissolved in 20 mL DIW to obtain a aqueous solution (named as solution C). Afterward, solution A was injected into solution B, forming a light pink turbid liquid, then followed by dropwise addition of solution C. After stirring for 1 h, 20 mL of NaOH solution with a high concentration of 8 mol $L^{-1}$ was dropped in the above suspension liquid with successive stirring for 20 min. Finally, $CoSn(OH)_6$ precipitates were then separated by centrifugation, washed with DIW/EA several times and dried at 80 °C for 12 h.

**Preparation of $CoSn(OH)_6$@polydopamine (PDA) nanocubes:** 150 mg of the obtained $CoSn(OH)_6$ powerd was added in a Tris-buffer(1.2114g in 50mL DIW + 50mL EA) under ultrasonic dispersion for 20 min. Then, 200 mg dopamine hydrochloride power was mixed, and the solution was kept stirring for 24h. Finally, the black $CoSn(OH)_6$@PDA powder was obtained after washing and drying in oven at 80 °C for 12 h.

**Preparation of Sn-Co@C nanocubes:** The as-prepared $CoSn(OH)_6$@PDA powder was annealed at 650 °C (heating rate: 2 °C $min^{-1}$) under $H_2$(5%)/Ar(95%) atmosphere for 5 h. Then, the black Sn-Co@C powder was obtained.

**Preparation of Sn-Co@C nanocubes:** The Sn-Co sample preparation process is similar to Sn-Co@C, including $CoSn(OH)_6$ nanocubes preparation. The as-prepared $CoSn(OH)_6$ powder was annealed at 650 °C (heating rate: 2 °C $min^{-1}$) under H2(5%)/Ar(95%) atmosphere for 5 h. Then, the blue Sn-Co powder was obtained.

**Preparation of Sn-Co@C and Sn-Co on the Cu current collector:** Commercial Cu foil was used as substrate to prepare the Sn-Co@C current collectors. The obtained Sn-Co@C powder was mixed with PVDF (mass ratio: 9:1) in N-Methyl pyrrolidone (NMP) solvent. Afterwards, the slurry was coated on 2D Cu foil via doctor blade and dried at 80 °C for 12 h. The mass loading of Sn-Co@C is about 1 mg $cm^{-2}$.

**Material characterization:** The morphologies and structures of materials were detected via scanning electron microscope (SEM, JEOL JSM-7610FPlus) and transmission elactron microscopy (TEM, JEOL JEM-F200). Crystalline structures of samples were measured by X-ray diffraction (XRD, Rigaku-TTR III) with Cu-K α radiation. The superficial elemental analyses of $CoSn(OH)_6$ and Sn-Co@C nanoparticles were performed by X-ray photoelectron spectroscopy (XPS, Thermo Scientific K-Alpha). The appropriate calcination temperature of Sn-Co@C nanoparticles was determined via thermogravimetric analysis under air atmosphere (TGA, SDT-Q600). Raman spectra were acquired utilizing LabRAM HR800 (HORIBA Jobin Yvon). And pore structure information was collected via nitrogen adsorption/desorption using a JWGB volumetric gas adsorption apparatus at 77 K.

**Electrochemical measurement:** CR2016 coin cells were assembled with Li foils, Celgard separator and the above-mentioned Sn-Co@C disks or commercial Cu foil in Ar-filled glovebox (water and oxygen content: <0.1 ppm). 1 M bis(trifluoromethane) sulfonamide lithium salt (LiTFSI) and solvent of 1, 3-dioxolane (DOL) and 1, 2-dimethoxyethane (DME) (v/v, 1:1) with 2wt% $LiNO_3$ additive as electrolyte were added to test cells. To evaluate the CE, metallic Li (1 mAh $cm^{-2}$) was plated on different current collectors at 1 mA $cm^{-2}$ and stripped away for charging to 1 V. To investigate the symmetric cells, working electrodes were prepared by first electroplating 5 mA h $cm^{-2}$ Li metal at 0.5 mA $cm^{-2}$, and then cycling at different current density and capacity. For testing the performance of full cells, 5 mAh $cm^{-2}$ of Li was pre-deposited on the disks as the anode, which paired with $LiFePO_4$ (LFP) cathode (loading of the active material was about 8~9 mg $cm^{-2}$). The cathode was prepared by mixing LFP powder (80 wt %), polyvinylidene fluoride binder (PVDF) (10 wt %) and super P (10 wt %) with mass ratio of 8:1:1. These full cells were galvanostatically cycled between 2.5 and 4 V (1C=170 mA $g^{-1}$ ).

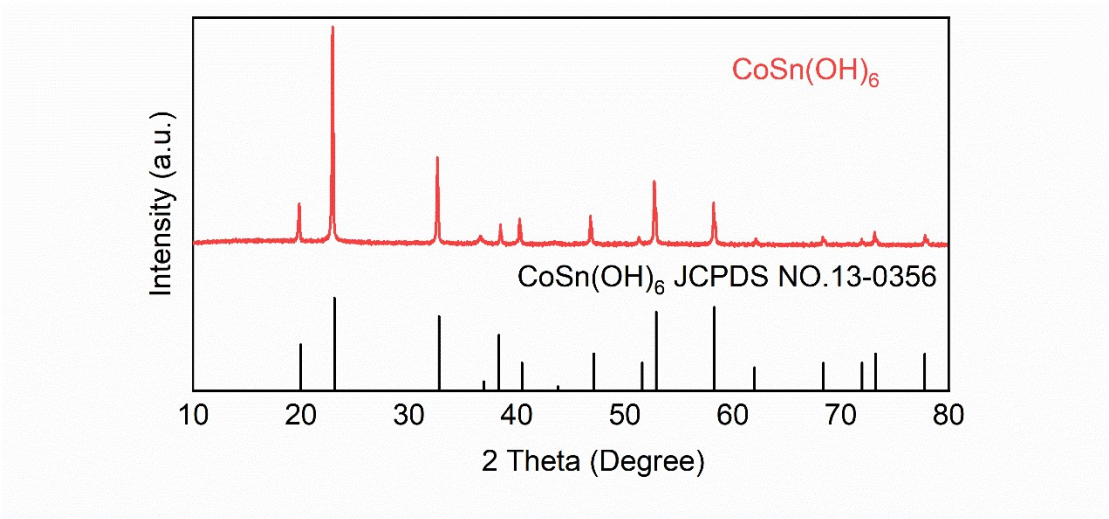


Fig. S1. The XRD pattern of $CoSn(OH)_6$ precursor.

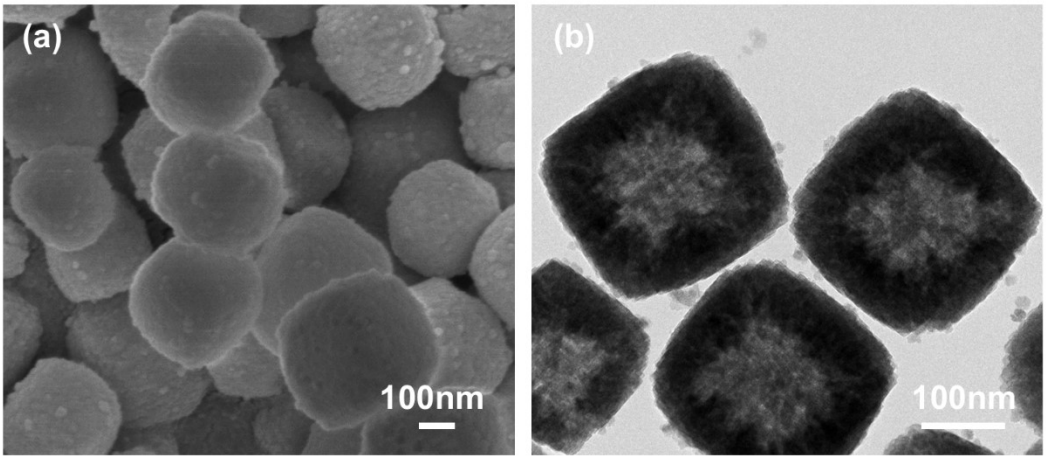


Fig. S2. (a) SEM and (b)TEM images of hollow $CoSn(OH)_6$ nanocubes.

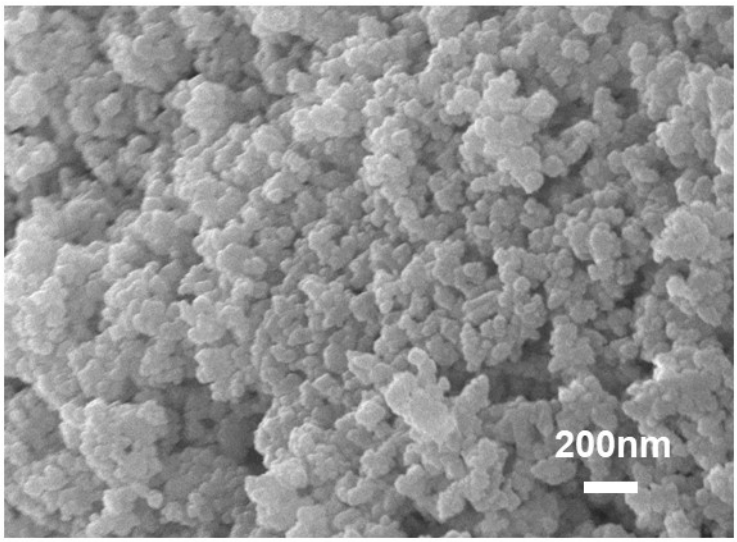


Fig. S3. SEM image of bare Sn-Co alloy.

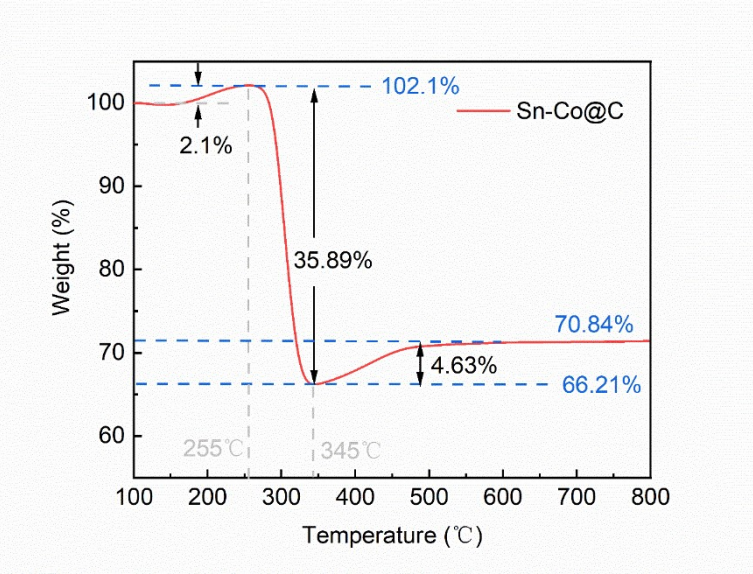


Fig. S4. TGA curves of Sn-Co@C sample.

According to the principle of mass conservation, the Sn-Co alloy component is eventually oxidized to $SnO_2$ and $Co_3O_4$ in air. The Sn-Co content can be roughly calculated as 51.82% according to the following equation, so the material carbon content is 48.18%.

$$\text{Sn - Co wt\%} = \frac{m_1}{M_{(SnO_2)} + {}^{1}/_{3}M_{(Co_3O_4)}} \times \frac{M_{(Sn\text{ - }Co)}}{m_0}$$

$m_0$=3.6983mg (mass weight of sample at 160°C after water removal)

$m_1$=2.6461mg (mass sample weight after TGA analysis)

$M(SnO_2)$ =150.7g $mol^{-1}$ (molecular weight of $SnO_2$)

$M(Co_3O_4)$ =284 g $mol^{-1}$ (molecular weight of $Co_3O_4$)

M(Sn-Co) =177.7 g $mol^{-1}$ (molecular weight of Sn-Co)

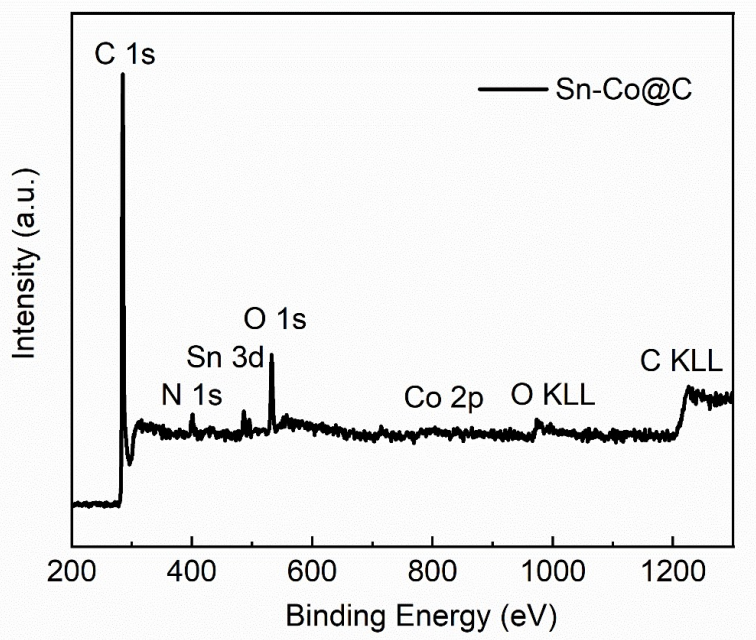


Fig. S5. Survey XPS spectra of Sn-Co@C sample.

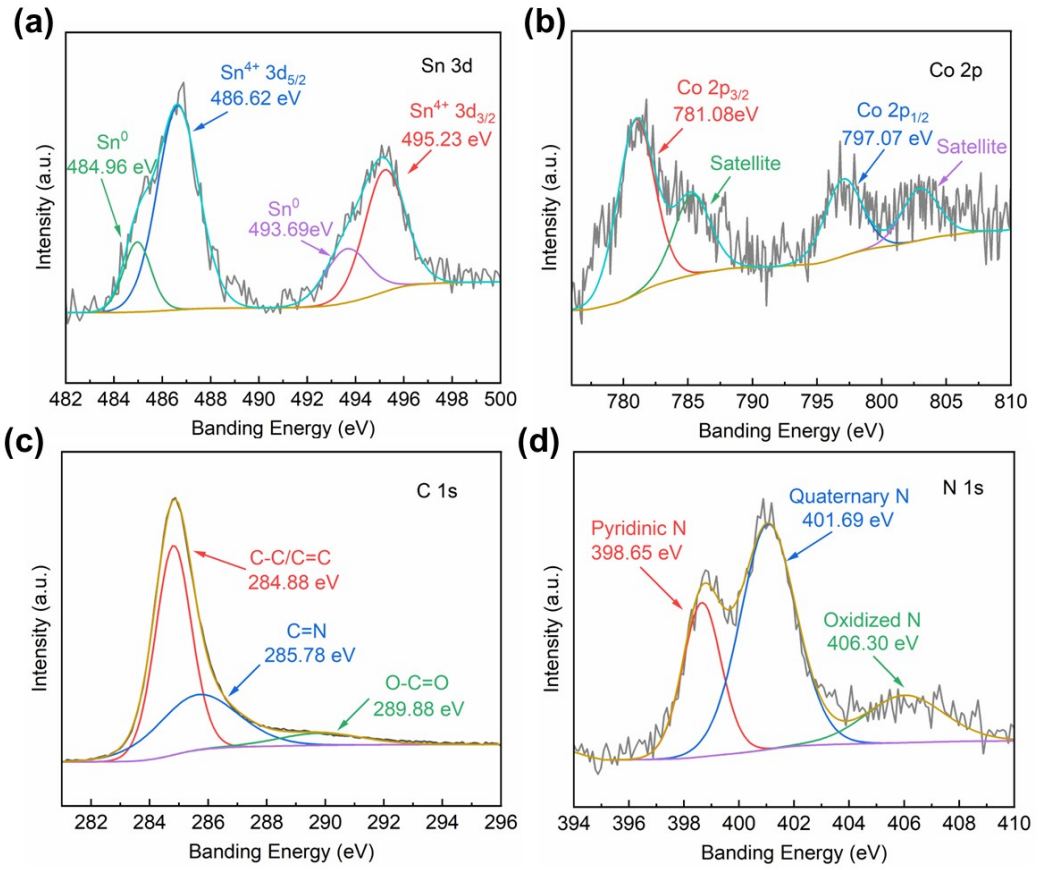


Fig. S6. High-resolution XPS spectra of Sn 3d (a), Co 2p (b), C 1s (c) and N 1s (d) of Sn-Co@C.

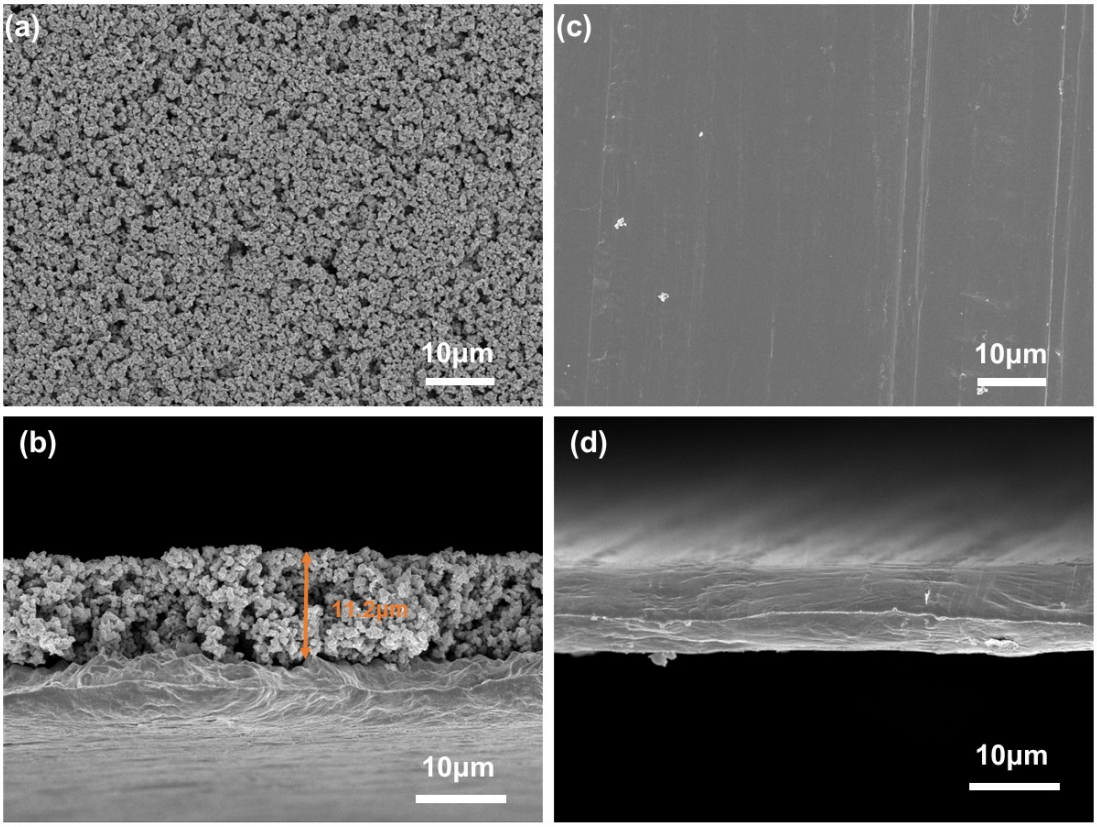


Fig. S7. (a, b) The SEM images of surface and cross-sectional morphologies Sn-Co@C current collector. (c, d) The SEM images of surface and cross-sectional morphologies bare Cu current collector.

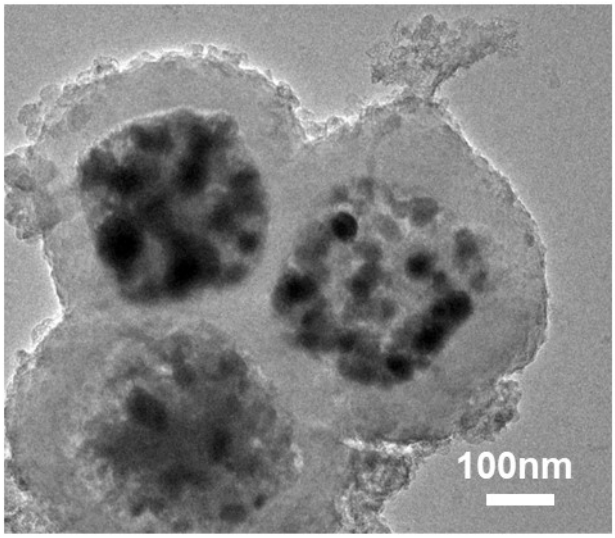


Fig. S8. TEM image of Sn-Co@C nanoparticles after 10 cycles at 1 mA $cm^{-2}$ and 1 mAh $cm^{-2}$.

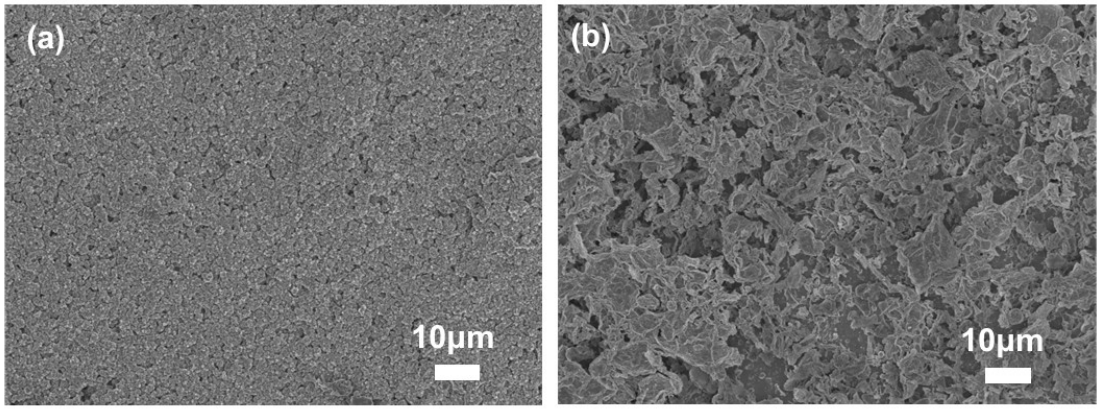


Fig. S9. The SEM images of stripping-state Sn-Co@C (a) and bare Cu (b) current after 10 cycles at 1 mA $cm^{-2}$, 1 mAh $cm^{-2}$.

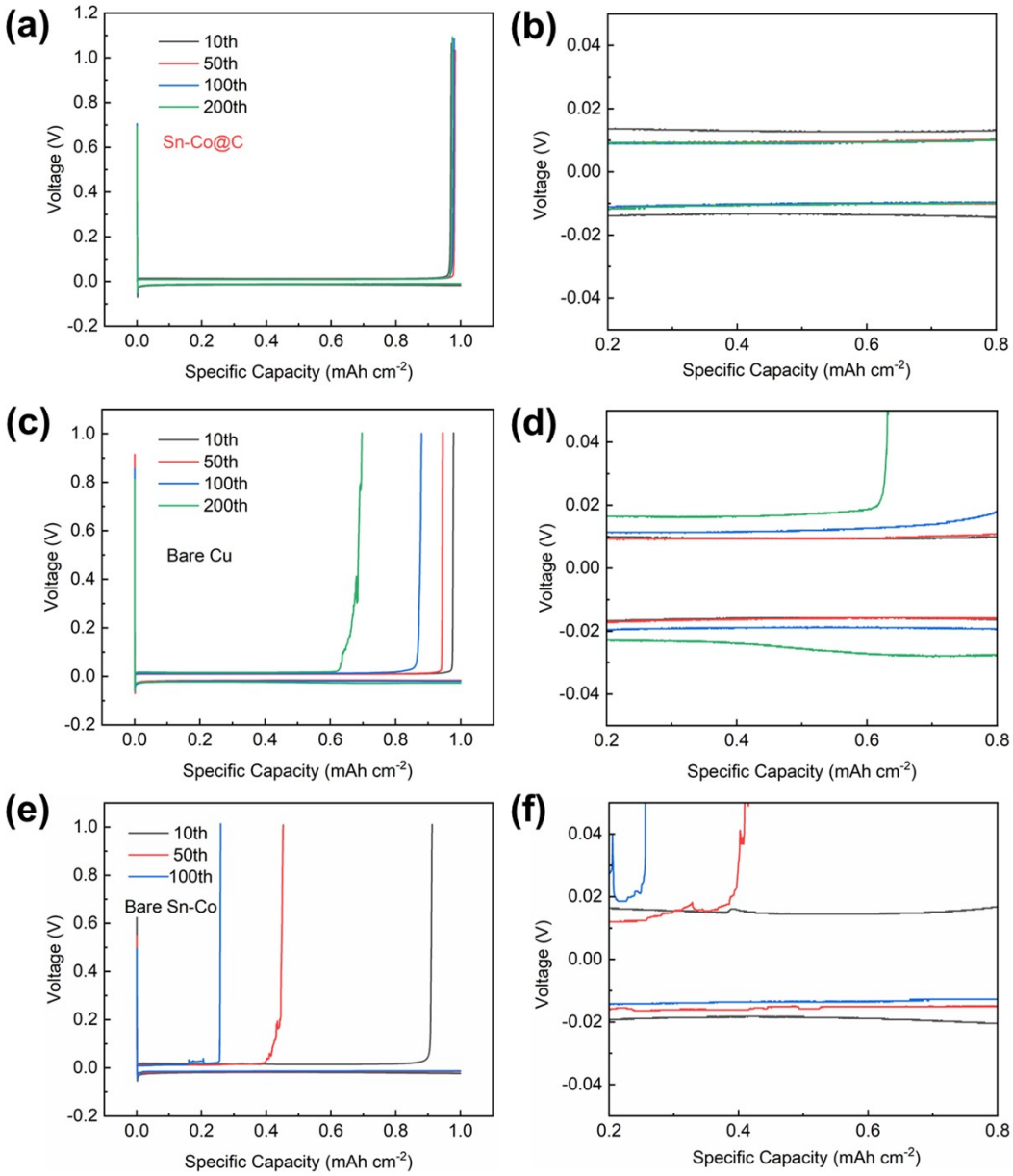


Fig. S10. The enlarged voltage profiles of Sn-Co@C (a,b), bare Cu (c, d) and bare Sn-Co (e, f) during Li cycling at the condition of 1 mA $cm^{-2}$ and 1 mAh $cm^{-2}$.

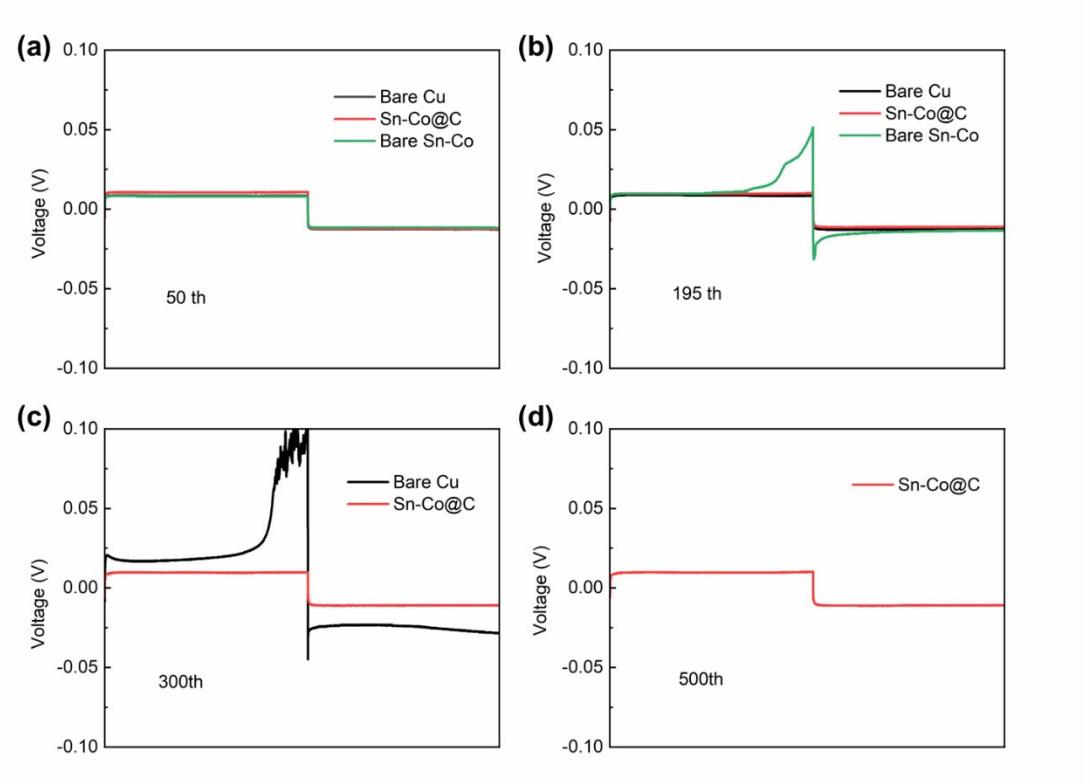


Fig. S11. The enlarged voltage profiles of bare Cu, bare Sn-Co and Sn-Co@C-based symmetrical cells at 1 mA $cm^{-2}$ and 1 mAh $cm^{-2}$ for 50th (a), 195th (b), 300th (c), 500th (d).

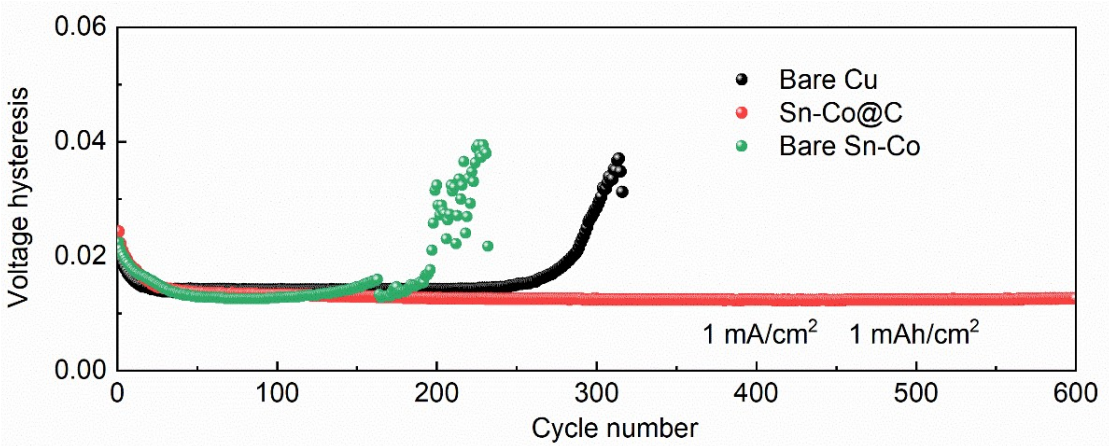


Fig. S12. The voltage hysteresis comparison of bare Cu, bare Sn-Co and Sn-Co@C-based symmetric cells under the conditions of 1 mA $cm^{-2}$ and 1 mAh $cm^{-2}$.

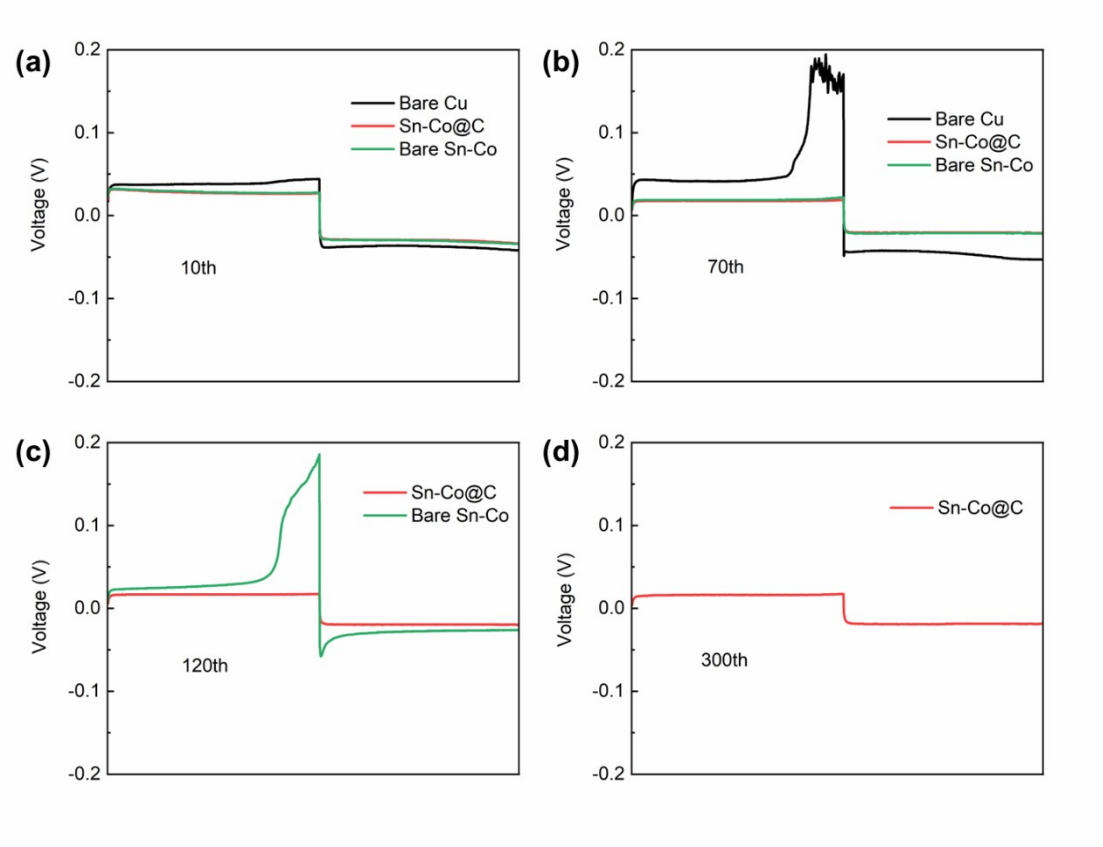


Fig. S13. The enlarged voltage profiles of bare Cu, bare Sn-Co and Sn-Co@C-based symmetrical cells at 5 mA $cm^{-2}$ and 1 mAh $cm^{-2}$ for 10th (a), 70th (b), 120th (c), 300th (d).

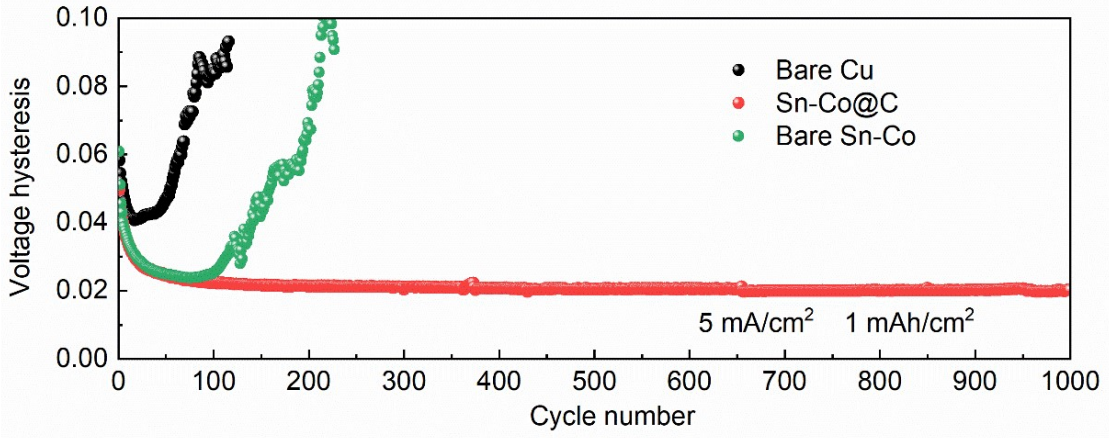


Fig. S14. The voltage hysteresis comparison of bare Cu, bare Sn-Co and Sn-Co@C-based symmetric cells under the conditions of 5 mA $cm^{-2}$ and 1 mAh $cm^{-2}$.

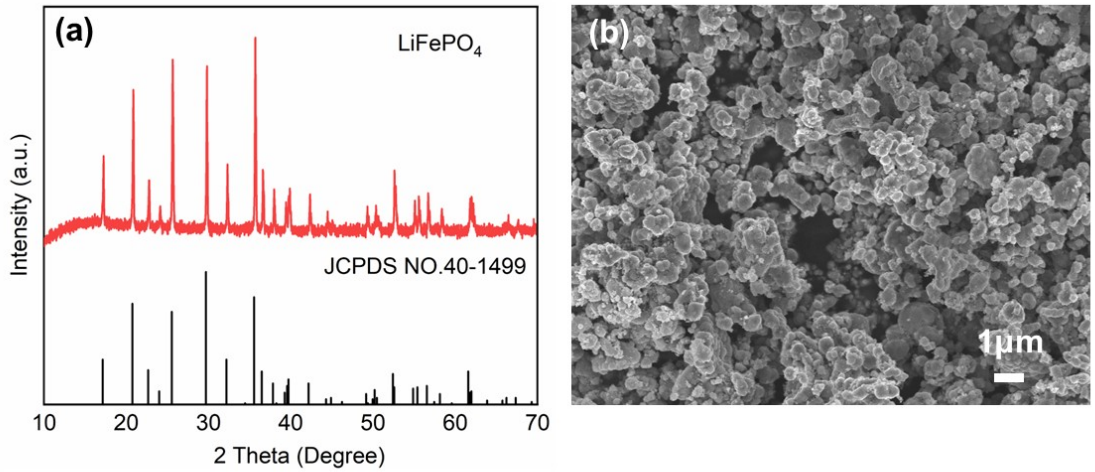


Fig. S15. The XRD pattern (a) and SEM image (b) of $LiFePO_4$.

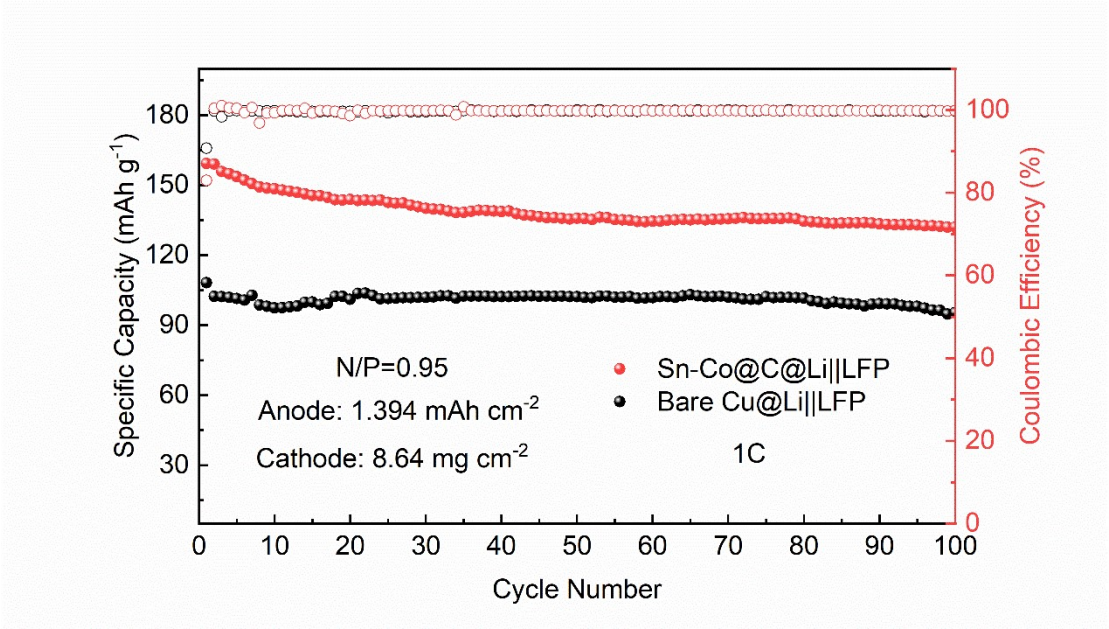


Fig. S16. Cycling performance of bare Cu@Li||LFP and Sn-Co@C@Li||LFP full cells at 1C.

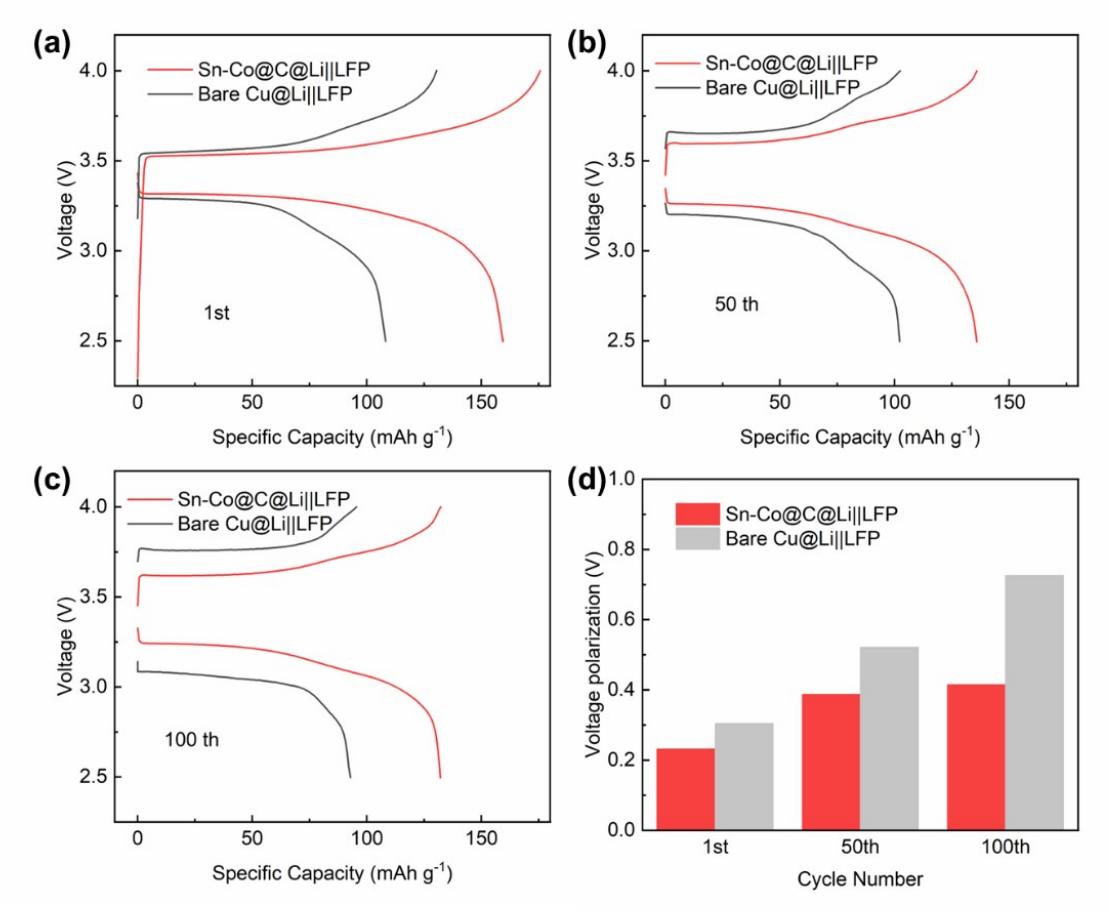


Fig. S17 Specific capacity-voltage profiles for 1st (a), 50th (b), 100th (c), and voltage polarization comparison (d) at 1C rate of bare Cu@Li||LFP and Sn-Co@C@Li||LFP full cells.

Table S1. Comparison of long-term cycling in symmetrical cells of different electrodes.

| Materials | Test condition | Time (h) | Ref. |
|---|---|---|---|
| CNT@SiOx-C. | 1 mA $cm^{-2}$, 1 mAh $cm^{-2}$ | 950h | [1] |
| CuS/$Cu_2S$@Cu | 1 mA $cm^{-2}$, 1 mAh $cm^{-2}$ | 880h | [2] |
| Dual-gradient Cu-Au-ZnO-PAN-ZnO | 1 mA $cm^{-2}$, 1 mAh $cm^{-2}$ | 600h | [3] |
| 3D Cu current collectors | 1 mA $cm^{-2}$, 1 mAh $cm^{-2}$ | 400h | [4] |
| Ni-Co hollow prisms@carbon fibers | 1 mA $cm^{-2}$, 1 mAh $cm^{-2}$ | 1200h | [5] |
| Co nanoparticles in N-graphene | 1 mA $cm^{-2}$, 1 mAh $cm^{-2}$ | 1000h | [6] |
| Zn@N-doped built on carbon cloth | 1 mA $cm^{-2}$, 1 mAh $cm^{-2}$ | 1200h | [7] |
| N-doped CNTs/Ni foam | 1 mA $cm^{-2}$, 1 mAh $cm^{-2}$ | 1000h | [8] |
| Au carbon fabric | 1 mA $cm^{-2}$, 1 mAh $cm^{-2}$ | 630h | [9] |
| Carbon cloth with SiC whiskers | 1 mA $cm^{-2}$, 1 mAh $cm^{-2}$ | 1000h | [10] |
| **Sn-Co@C** | **1 mA $cm^{-2}$, 1 mAh $cm^{-2}$**<br>**5 mA $cm^{-2}$, 1 mAh $cm^{-2}$** | **1350h**<br>**400h** | **This work** |

Table S2. Comparison of long-term cycling in full cells of different anodes.

| Modified anode materials | Test condition | N/P | Cycles | Ref. |
|---|---|---|---|---|
| $CuS/Cu_2S$@Cu | 1C | 5.2 | 200 | [2] |
| Ag-N-doped carbon nanoflake | 1C | / | 70 | [11] |
| 3D porous nitrogen doped carbon | 50 $mAg^{-1}$ | / | 50 | [12] |
| Ni-Co hollow prisms@carbon fibers | 1C | 6 | 150 | [5] |
| Co nanoparticles in N-graphene | 1C | / | 100 | [6] |
| Zn@N-doped built on carbon cloth | 1C | 5.2 | 160 | [7] |
| Au carbon fabric | 0.5C | / | 145 | [9] |
| carbon cloth with SiC whiskers | 0.5C | 4.4 | 120 | [10] |
| **Sn-Co@C** | **1C** | **2.12** | **250** | **This work** |

## References


[1] Z. Lu, S. Liu, C. Li, J. Huang, D. Wu, R. Fu, *Chem. Commun.* **2019**, 55, 6034.

[2] K. Lin, T. Li, S.-W. Chiang, M. Liu, X. Qin, X. Xu, L. Zhang, F. Kang, G. Chen, B. Li, *Small* **2020**, 16, 2001784.

[3] H. Zheng, Q. Zhang, Q. Chen, W. Xu, Q. Xie, Y. Cai, Y. Ma, Z. Qiao, Q. Luo, J. Lin, L. Wang, B. Qu, B. Sa, D.-L. Peng, *J. Mater. Chem. A* **2020**, 8, 313.

[4] H. Zhao, D. Lei, Y.-B. He, Y. Yuan, Q. Yun, B. Ni, W. Lv, B. Li, Q.-H. Yang, F. Kang, J. Lu, *Adv. Energy Mater.* **2018**, 8, 1800266.

[5] C. Chen, J. Guan, N. W. Li, Y. Lu, D. Luan, C. H. Zhang, G. Cheng, L. Yu, X. W. Lou, *Adv. Mater.* **2021**, 33, 2100608.

[6] T.-S. Wang, X. Liu, X. Zhao, P. He, C.-W. Nan, L.-Z. Fan, *Adv. Funct. Mater.* **2020**, 30, 2000786.

[7] L. You, S. Ju, J. Liu, G. Xia, Z. Guo, X. Yu, *J. Energy Chem.* **2022**, 65, 439.

[8] Z. Zhang, J. Wang, X. Yan, S. Zhang, W. Yang, Z. Zhuang, W.-Q. Han, *Energy Storage Mater.* **2020**, 29, 332.

[9] D. Li, Y. Gao, C. Xie, Z. Zheng, *Appl. Phys. Rev.* **2022**, 9, 011424.

[10] B. Sun, Q. Zhang, W. Xu, R. Zhao, H. Zhu, W. Lv, X. Li, N. Yang, *Nano Energy* **2022**, 94, 106937.

[11] Q. Sun, W. Zhai, G. Hou, J. Feng, L. Zhang, P. Si, S. Guo, L. Ci, *ACS Sustain. Chem. Eng.* **2018**, 6, 15219.

[12] A. Patrike, K. Suresh, M. Wahid, V. Chaturvedi, M. V. Shelke, *Carbon* **2021**, 179, 256.